Geometric Trajectory Planning for Robot Motion Over a 3D Surface

Bashir Hosseini Jafari, Nolan Walker, Ronald Smaldone, and Nicholas Gans

Abstract—Mapping a desired 2D pattern onto a curved surface has many applications. This includes motion planning for mobile robots to perform coverage path planing (CPP), robot end effector trajectory design for tasks such as printing, depositing, wielding on a 3D surface. This problem becomes more difficult if we want the mapped pattern to keep the properties of the original pattern (i.e, least possible mapping distortion), and pass over some desired points and/or remain bounded in a specific region on the surface. In this paper, we apply surface parametrization and mapping distortion analysis, which is rarely used in robot motion planning works, to map a pattern onto 3D surface. To meet additional goals such as passing over certain points, a planar mapping determined by constrained optimization is employed on the original pattern. Our focus is on printing/depositing materials on curved surfaces, and simulations and experiments are provided to confirm the performance of the approach.

I. Introduction

There are a number of tasks that require following a desired trajectory along a curved surface. Applications for mobile robots and UAVs include coverage path planning (CPP) [1]–[3], agricultural field automation [4], vacuum cleaning robots [5], lawn mowers [6], [7], etc. We are particularly interested in printing or jetting materials onto curved surfaces, with application in painting robots [8], [9], printing antennas, depositing lines with desired width [10] and automatic wound filling. Defining or mapping a specific trajectory to curved surfaces is challenging, and this challenge is increased when the trajectory must pass over specific points and/or remain bounded in a desired region.

In this paper, we apply surface parametrization, planar mapping and optimization to propose a novel approach to solve this problem. Surface parametrization is a mapping from a surface to the parametric domain. There has been work in the image processing and computer graphics community for tasks such as surface parametrization, including texture mapping modification, mesh editing [11] and completion [12]. However, the use of surface parametrization in robot path planning remains limited. To our knowledge, there is only one recent work considering surface parametrization for motion planning [13]; this work focuses on surface parameterization for CPP, but the result considers only mapping

This material is based upon work supported by the National Science Foundation under Grant No. 1563424,

N. Gans is a member of UT Arlington Research Institute, The University of Texas at Arlington, Fort Worth. Other authors all are at University of Texas at Dallas, Richardson, Texas. B. Jafari is member of the Department of Electrical and Computer Engineering; N. Walker is a Member of the Department of Mechanical Engineering; R. Smaldone is a member of the Department of Chemistry. {bxh140430, Nolan.Walker, Ronald.Smaldone}@utdallas.edu, ngans@uta.edu.

the boustrophedon decomposition. Our work is capable of mapping any parameterized 2D curve to a 3D quadric surface and employs a different mapping approach compared to [13]. We also investigate different possible mappings to get the minimum possible distortion, depending on the surface. In addition, there is no surface decomposition/partitioning in this work.

In this work, by applying surface parametrization and minimizing map distortion, we map designed patterns in 2D onto 3D quadric surfaces. This pattern can be arbitrary, but it must be parametrized by one independent variable in a continuous function. By applying an affine transformation on the original 2D pattern, found via constrained optimization, we meet additional goals such as visiting way points on the surface and ensuring desired bounds for the pattern.

Surface parametrization can be considered as a mapping from a surface to a parametric domain in lower dimensions. This parametrization allows us to move from parameter surface to a 3D space. Surfaces that are homomorphic to a disk have a parameter space in the 2D plane. This concept lets us map a pattern in 2D to a geometric shape in 3D space. This projection might result in distortion in either angle or area. As we want to follow the same pattern on the surface as it is designed in 2D, isometric (length preserving) and conformal (angle preservative) projections are desirable to minimize distortion. This motion problem, constrained to some conditions, can be also viewed as curve fitting on a manifold, provided that there are enough desired 3D points on the surface to determine the pattern.

The paper proceeds as follows. Section II presents mathematical background about modeling, surface/curve parametrization and differential geometry. Section III presents how to map a planar patten onto a curved surface with some conditions. In section IV, we apply curve fitting method for a set of points on the manifold to generate a pattern on a 3D surface. Simulations are presented throughout Sections III and IV, and experiments using a 3D printer are presented in Section V.

II. MATHEMATICAL PRELIMINARIES

A. Quadric Surfaces and Modeling

A surface S is the set of points $[x,y,z] \in \mathbb{R}^3$ that satisfy an implicit equation of the form f(x,y,z)=0 and can be parametrized by two independent variables. In other words, a surface is a deformed plane that is considered as a two dimensional manifold.

In this work, we limit our consideration to surfaces that can be categorized as orientable topological surfaces with boundary. Thus, every point has an open neighborhood homeomorphic to an open subset of the Euclidean plane. Furthermore, the surface will admit a Riemannian metric. We focus on quadric surfaces, which have the implicit function of the form

$$Ax^{2} + By^{2} + Cz^{2} + 2Dxy + 2Exz + 2Fyz + 2Gx + 2Hy + 2Iz + 2J = 0$$
 (1)

where A, \ldots, J are coefficients of the surface equation and determine the geometric shape, location and orientation of the quadric surfaces. Examples of quadric surfaces includes spheres, ellipsoids and cones. Coefficient A, \ldots, J can either be determined by the point clouds of the surface or geometric characteristics like center, radius, axis. In this paper, we assume the quadric surface model is given and it is in standard form, which we will discuss in section III.C. In case where quadric surfaces are not in standard equation, coordinate transformation can be applied to convert them to standard form.

B. Curve and Surface Parametrization

The map $r_s(u,v) = [x(u,v),y(u,v),z(u,v)]$ defines a surface parametrization, where $r_s \in \mathbb{R}^3$ and $[u,v] \in \mathbb{R}^2$. The surface is defined by three functions x(u,v),y(u,v),z(u,v); each is a function of two variables u and v. The image of $r_c(\theta) = [x(\theta),y(\theta),z(\theta)]$ from parameter $\theta \in \mathbb{R}$ to a curve $r_c \in \mathbb{R}^3$, is called curve parametrization. 2D curve parametrization is written as $r_{cp}(\theta) = [u(\theta),v(\theta)]$, where $r_{cp} \in \mathbb{R}^2$.

C. Differential Geometry Background

To be able to apply the usual notation of calculus on a surface, we introduce the definition of a regular surface [14]. Consider a surface $S \subset \mathbb{R}^3$ with parametric representation

$$r_s(u, v) = [x(u, v), y(u, v), z(u, v)]$$
 (2)

for points [u,v] in some domain in \mathbb{R}^2 . This representation is regular if for each $p \in S$, there exist a neighborhood $V \subset \mathbb{R}^3$ and a map $r_s: U \to V \cap S$ of an open set $U \subset \mathbb{R}^2$ onto $V \cap S \subset \mathbb{R}^3$ such that

- 1) x(u,v), y(u,v), z(u,v) have continuous partial derivatives of all orders in U.
- 2) r_s is a homeomorphism.
- 3) For each $q \in U$, the differential $dr_s : \mathbb{R}^2 \to \mathbb{R}^3$ is one-to-one.

Before proceeding, to be capable to calculate metric properties of a regular surface, the first fundamental form (I) is introduced. It allows us to make measurements such as length of curves, area of regions, angle between curves, etc. on the surface. These measurements allow us to compare different mappings. For example, a mapping from one surface to another that preserves the length of curves between mapped points is of interest.

Many properties of S are characterized by its first fundamental form. The arc length of a curve in \mathbb{R}^3 is equal to

$$ds^{2} = X_{1} \cdot X_{1}(du)^{2} + 2X_{1} \cdot X_{2}dudv + X_{2} \cdot X_{2}(dv)^{2}$$
 (3)

where $X_1 = \partial r_s/\partial u$, $X_2 = \partial r_s/\partial v$. Encapsulating the coefficients in a symmetric matrix I, we have

$$ds^{2} = \begin{pmatrix} du & dv \end{pmatrix} \mathbf{I} \begin{pmatrix} du \\ dv \end{pmatrix} \tag{4}$$

where

$$\mathbf{I} = \begin{pmatrix} X_1 \cdot X_1 & X_1 \cdot X_2 \\ X_2 \cdot X_1 & X_2 \cdot X_2 \end{pmatrix}. \tag{5}$$

In the following, we introduce useful mappings based on discussion in [15].

D. Isometric Mapping

A mapping from metric space M to metric space N is isometric or length-preserving if the length of any arc on N is the same as that of its original on M.

Theorem 1. A mapping from surface S_1 to S_2 is considered isometric if and only if there exist parametrization $r_s: U \to S_1 \subseteq \mathbb{R}^3$ and $r_s': U \to S_2 \subseteq \mathbb{R}^3$ with the same first fundamental form, i.e

$$\mathbf{I}_{r_s} = \mathbf{I}_{r'_s}.\tag{6}$$

E. Conformal Mapping

A mapping from metric space S_1 to S_2 is conformal or angle-preserving if it preserves local angles as well as orientation. This mapping does not necessarily preserve size or curvature.

Theorem 2. A mapping from surface S_1 to S_2 is conformal or angle preserving if and only if there exist parametrization $r_s: U \to S_1 \subseteq \mathbb{R}^3$ and $r_s': U \to S_2 \subseteq \mathbb{R}^3$ with the first fundamental forms are proportional, i.e

$$\mathbf{I}_r = \eta \ \mathbf{I}_{r'},\tag{7}$$

for scalar function $\eta \neq 0$.

F. Equiareal Maps

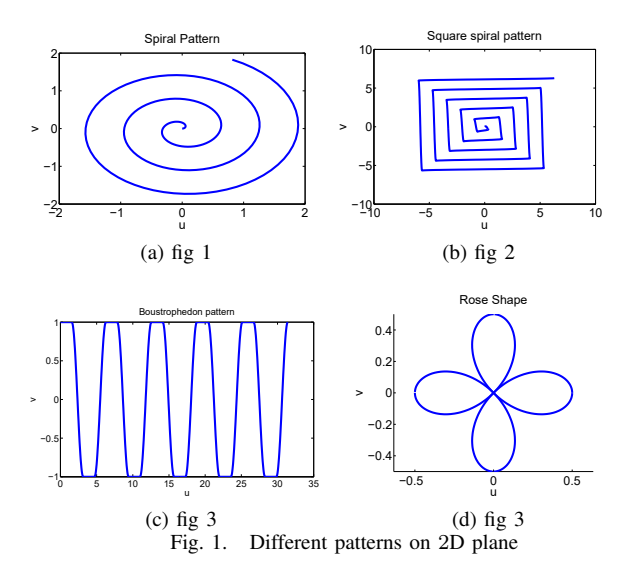
A mapping from surface S_1 to S_2 is equiareal if it preserves the area of any section.

Theorem 3. A mapping from S_1 to S_2 is equiareal if and only if the determinant of the first fundamental forms are equal, i.e.

$$\left|\mathbf{I}_{r}\right| = \left|\mathbf{I}_{r'}\right|.\tag{8}$$

Every isometric mapping is conformal and equiareal, and every conformal and equiareal mapping is isometric. An isometric mapping is ideal, because it preserves angles, areas, and lengths. However, isometric mappings only exist for a few surfaces.

Definition 1. A surface is called developable if it is smooth and its Gaussian curvature is zero. In other words, it is a surface that is obtained by deforming a plane without folding.



III. MAPPING 2D CURVES TO 3D SURFACE

Often the curve or path to be followed is first designed on a planar surface and must be mapped to the 3D surface. For example, back and forth motions (also known as Boustrophedon or lawn-mower path [16]) and spirals are common choices for coverage problems in the plane. In this work, we are planning the path or trajectory, which can then be carried out by any robot using the forward kinematics. Successful path generation will require a mapping with the least amount of distortion to preserve the properties of the path. Given the implicit equation describing the surface, tools of differential geometry can find a mapping between a curve in the plane and a curve on the surface. The mapping r_s must have minimal distortion, so we will focus on isometric mappings, which preserve length, and conformal mappings, which preserve angles between any pair of arcs. Developable surfaces, including planes, cylinders, tori and cones, admit an isometric map. For nondevelopable surfaces, we will focus on finding an alternative mapping. In this section, first, we parametrize the planar curve (pattern) in 2D. Second, we apply a planar mapping consisting of an affine transformation. The transformation parameters in the planar transformation can be tuned via optimization to let the pattern fulfill more tasks, such as passing over desired way points. Third, we find an appropriate mapping from a plane to a given surface with least amount of distortion.

A. Curve Parametrization

In this subsection, parametrization of some popular curve patterns are introduced, where $\alpha, \omega \in \mathbb{R}$ are constant and $\theta \in [b_1, b_2] \in \mathbb{R}$ is parametrization variable.

Spiral: $r_{cp}(\theta) = \alpha \theta [\cos(\omega \theta), \sin(\omega \theta)]$

Square spiral: $r_{cp}(\theta) = \alpha \theta [|\cos(\omega \theta)|\cos(\omega \theta) + |\sin(\omega \theta)|\sin(\omega \theta), |\cos(\omega \theta)|\cos(\omega \theta) - |\sin(\omega \theta)|\sin(\omega \theta)]$ Boustrophedon path: $r_{cp}(\theta) = \alpha [\omega t, |\cos(\omega \theta)|\cos(\omega \theta) + |\sin(\omega \theta)|\sin(\omega \theta)]$

Rose: $r_{cp}(\theta) = \alpha[\cos 2\theta \cos \theta, \cos 2\theta \sin \theta]$.

Fig. 1 shows each aforementioned pattern.

B. Planar Mapping

We perform a planar mapping transformation via matrix $K \in \mathbb{R}^{3 \times 3}$ from the original parameterized curve $r_{cp}(\theta)$, to a new parametrized curve, $r_{mp}(\theta) \in \mathbb{R}^2$. This mapping can be introduced in homogeneous coordinates as

$$\begin{bmatrix} r_{mp}(\theta) \\ 1 \end{bmatrix} = K \begin{bmatrix} r_{cp}(\theta) \\ 1 \end{bmatrix}$$

$$K = \begin{bmatrix} M & T \\ 0 & 1 \end{bmatrix}$$
(9)

where $M \in \mathbb{R}^{2 \times 2}$ accounts for transformations such as rotation, scaling, shear, etc and $T \in \mathbb{R}^2$ represents translation. The elements of K need to be optimized to satisfy extra goals. This optimization is explained in section III.D. After planar mapping, the next task is to map the planar mapped pattern to a 3D surface with the least possible distortion.

C. Mapping from 2D to 3D

Let S be a surface in \mathbb{R}^3 . It is desired to find a parametrization $r_s(u,v):\mathbb{R}^2\to S\in\mathbb{R}^3$ to map a 2D pattern onto a surface with the least possible distortion. Here, we discuss some famous quadric surfaces and how a 2D pattern can be best mapped to them.

1) Cylinder: The cylinder with implicit function

$$x^2 + y^2 = a^2 (10)$$

is a developable surface (zero Gauss curvature), and there is an isometric map between the (u,v) plane and cylinder

$$r_s(u, v) = [a\cos v, a\sin v, u] \tag{11}$$

where a determines the cylinder radius.

2) Torus: The torus is not a quadric surface, but it does have an implicit function and can be treated in our approach. The equation in Cartesian coordinates for a torus symmetric about *z*-axis is

$$(c - \sqrt{x^2 + y^2})^2 + z^2 = a^2 \tag{12}$$

where r = c - a and R = c + a are the inner and outer radii. The torus is also a developable surface, and there is an isometric map between the (u, v) plane and torus as

$$r_s(u, v) = [(c + a\cos v)\cos u, (c + a\cos v)\sin u, a\sin v].$$
(13)

3) Paraboloid: The implicit function of a paraboloid with z-axis as axis of symmetry and crossing [0, 0, 0] is

$$z = \frac{x^2}{a^2} + \frac{y^2}{b^2} \tag{14}$$

where its cross section is an ellipse with a and b as semi-major and semi-minor axes. The paraboloid is not a developable surface. However, it can be parametrized as

$$r_s(u, v) = [a\sqrt{u}\cos(v), b\sqrt{u}\sin(v), u]. \tag{15}$$

4) Sphere: The implicit function of a sphere centered at (0,0,0) with radius R in Cartesian coordinate is

$$x^2 + y^2 + z^2 = R^2. (16)$$

The sphere is not a developable surface, however, there is a conformal mapping (Stereographic projection) as

$$r_s(u,v) = \left[\frac{2uR^2}{R^2 + u^2 + v^2}, \frac{2vR^2}{R^2 + u^2 + v^2}, \frac{u^2 + v^2 - R^2}{R^2 + u^2 + v^2}R\right]. \tag{17}$$

The well-known spherical transformation

$$r_s(u, v) = [a \sin u \sin v, a \cos u \sin v, a \cos v]$$
 (18)

is neither conformal nor isometric.

5) Ellipsoid: The implicit function of the ellipsoid in a Cartesian coordinate system is

$$\frac{x^2}{a^2} + \frac{y^2}{b^2} + \frac{z^2}{c^2} = 1. {19}$$

There is a conformal map named Mercator given by

$$r_s(u, v) = [a \operatorname{sech} v \cos u, b \operatorname{sech} v \sin u, c \tanh v)].$$
 (20)

6) Cone: An elliptic cone Cartesian coordinates function is

$$\frac{x^2}{a^2} + \frac{y^2}{b^2} = z^2 \tag{21}$$

which has a locally isometric surface parametrization

$$r_s(u, v) = [au\cos v, bu\sin v, u]. \tag{22}$$

D. Pattern Placement Via Optimization

In the previous section, we discussed the map of interest that renders least amount of distortion from plane to an specific surface. In addition to this goal, we want to place our 2D pattern on a desired location on the surface. For example, we want the pattern to pass through a specific set of via points on the surfaces or limit it in a box with boundaries. To address this additional purpose, we optimize K in (9). Before proceeding, we define \hat{r}_s by removing one element of r_s , depending on the objective function.

1) Pattern With Boundary: The goal in this case is to locate the pattern inside some desired boundaries. Define $r_{max}, r_{min} \in \mathbb{R}^2$ as the maximum and minimum desired values of z and y respectively. We want $\max(\hat{r}_s(r_{mp}(\theta))) = r_{max}$, and $\min(\hat{r}_s(r_{mp}(\theta))) = r_{min}$ for any $\theta \in [b_1, b_2]$. By tuning K, the pattern $r_{cp}(\theta)$ can be contracted/stretched or shifted, sheared , translated, etc in the 2D by K such that it lies on the desired place of the surface. The optimization problem can be defined as follows

$$min(||K||^{2})$$

$$s.t: max(\hat{r}_{s}(r_{mp}(\theta)) = r_{max}$$

$$min(\hat{r}_{s}(r_{mp}(\theta)) = r_{min}.$$
(23)

Because the pattern is mapped on a surface, by confining two dimensions, the third dimension would automatically be confined based on the surface function. That is why \hat{r}_s is used rather than r_s in (23). In Fig. 2, we simulated

a pattern placement on a cylinder. The cylinder equation is given in (10), with a=1. The original pattern is a spiral, with $\alpha=1, \omega=2, \theta\in[0,6\pi]$, and the mapping from 2D to 3D, $r_s(u,v)$, is based on (11) with a=1. The desired limits are $r_{max}=[z_{max}\;y_{max}]=[2\;1]$ and $r_{min}=[z_{min}\;y_{min}]=[-1\;0.5]$. K is optimized in Matlab using fmincon/fminsearch with different initial values that all converge to the same final value. The results in Fig. 2 shows a) spiral pattern is successfully mapped to the cylinder with minimal distortion, b) the pattern after affine transformation, $r_{mp}(\theta)$, where K was optimized to locate the pattern inside the boundary and c) ZY coordinates of the 3D pattern on the cylinder. It can be observed that the max and min values are the desired values.

We define three error metrics. The first two, E_i , E_c represents isometric and conformal mapping errors respectively. They are given by

$$E_i = \sum_{i,j=1}^{n} (d(r_s(r_{cp}(\theta_i)), r_s(r_{cp}(\theta_j))) - d(r_{cp}(\theta_i), r_{cp}(\theta_j)))^2$$

$$E_{c} = \sum_{i,j=1}^{n} (\angle(r_{s}(r_{cp}(\theta_{i})), r_{s}(r_{cp}(\theta_{j}))) - \angle(r_{cp}(\theta_{i}), r_{cp}(\theta_{j})))^{2}.$$
(24)

where \angle and d mean angle and arc length. Errors are measured during optimization, $E_i \approx 10^{-7}$ cm, $E_c \approx 10^{-8}$ rad, which is close to zero as expected (because (11) is an isometric and conformal parametrization). The condition error, which is sum of the squared error (SSE) of the optimization constraints is $E_{cd} \approx 10^{-5}$ cm, as the tolerance error for conditions in the fmincon algorithm was set to 10^{-5} .

E. Pattern Constrained to Pass Through Way Points

Given a set of way points p_i , i=1,...,n, on the surface, we might wish that the mapped pattern should pass through them. In other words, we not only want to impose the pattern structure (designed in 2D) on the surface, but that pattern should visit some check points on the 3D surface. For example, these points can be some positions that a robot needs to stop to collect some data, or to ensure that the robot would avoid obstacles. The optimization algorithm can be formulated as

$$\min(||K||^2)$$

$$s.t: \sum_{i=1}^{n} \min(||r_s(r_{mp}(\theta)) - p_i)||^2) = 0.$$
(25)

Fig. 3 shows the pattern mapped to the paraboloid (14), where a=b=1. This pattern is square spiral, with $a=1,\omega=5$ and $\theta\in[0.4\pi]$. The desired points to pass are

$$\begin{bmatrix} 1.64 \\ -0.525 \\ 2.97 \end{bmatrix} \begin{bmatrix} 1.63 \\ 0.543 \\ 2.98 \end{bmatrix} \begin{bmatrix} 1.14 \\ -0.034 \\ 1.3 \end{bmatrix} \begin{bmatrix} 1 \\ 0.28 \\ 1 \end{bmatrix}.$$

Fig. 3 depicts a) spiral pattern successfully mapped onto a paraboloid and passes through the desired way points with calculated condition error $E_{cd} \approx 10^{-4} cm$, b) the square

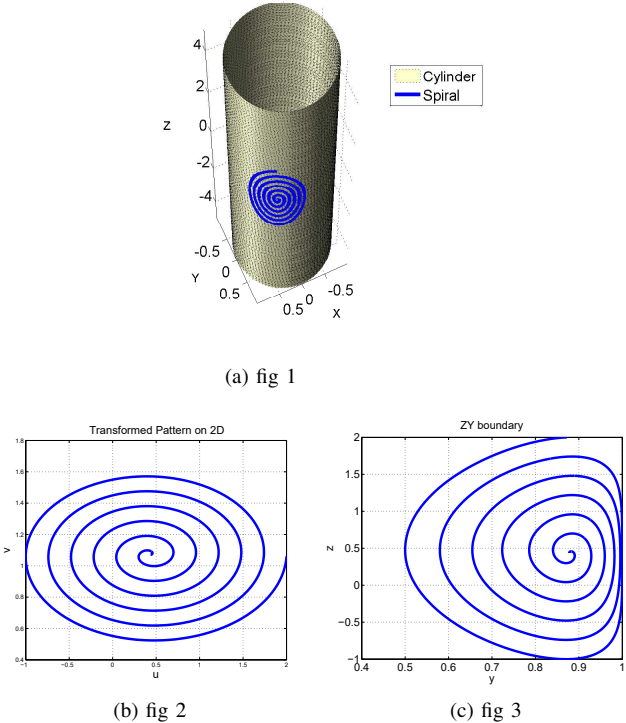


Fig. 2. Pattern placement of a spiral on a cylinder with boundary condition

spiral pattern after affine transformation, $r_{mp}(\theta)$, and c) ZY coordinates of the 3D pattern.

F. Pattern with Boundary to Pass Visiting Points

Here, we combine our previous objective function to define our ultimate goal. The pattern max and min boundary is set to a fixed desired value, and inside that boundary box, our pattern should pass through desired points on the surface. The optimization can be formulated as

$$\min(||K||^{2})$$

$$s.t: \sum_{i=1}^{n} \min(||r_{s}(r_{mp}(\theta)) - p_{i})||^{2}) = 0$$

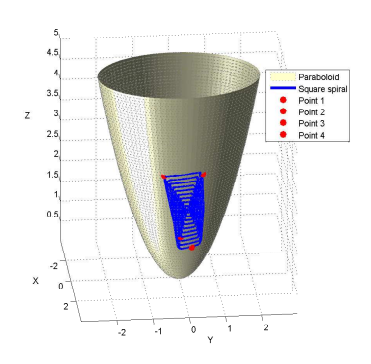
$$\max(\hat{r}_{s}(r_{mp}(\theta)) = r_{max}$$

$$\min(\hat{r}_{s}(r_{mp}(\theta)) = r_{min}.$$
(26)

We simulate a case where there is a cone based on (21), with a=b=1. A square spiral pattern with parameters $a=1,\omega=5$, and $\theta\in[0\ 4\pi]$ is defined. The task is to tune K to let the pattern pass through the following points

$$\begin{bmatrix} 2.16 \\ -0.67 \\ 2.27 \end{bmatrix} \begin{bmatrix} 2.157 \\ 0.907 \\ 2.34 \end{bmatrix} \begin{bmatrix} 0.932 \\ -0.544 \\ 1.08 \end{bmatrix} \begin{bmatrix} 1.155 \\ 0.393 \\ 1.22 \end{bmatrix} \begin{bmatrix} 1.602 \\ 0.37 \\ 1.64 \end{bmatrix} \begin{bmatrix} 1.558 \\ -0.341 \\ 1.595 \end{bmatrix}$$

and the desired extremum values of the pattern are $r_{max} = [z_{max} \ y_{max}] = [2.8 \ 1.4]$ and $r_{min} = [z_{min} \ y_{min}] = [1.07 \ -0.67]$. Fig. 4 shows a) pattern placement on the cone that successfully visits all desired points b) square spiral patten after the optimized affine transformation, and c) ZY coordinates of the mapped pattern. It can be observed that the max and min values are the same as the desired ones.



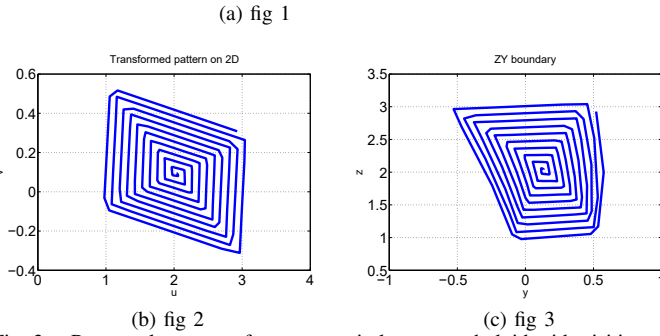


Fig. 3. Pattern placement of a square spiral on a paraboloid with visiting points condition

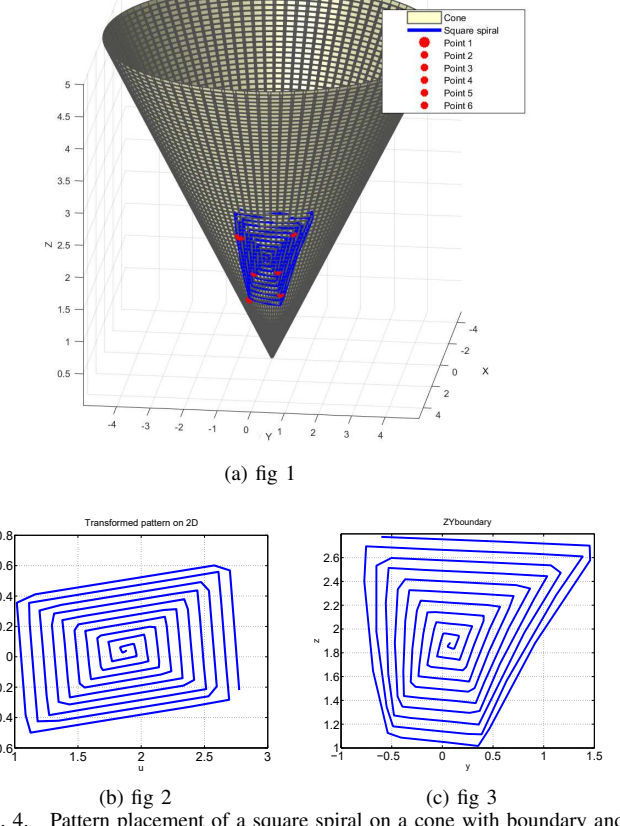
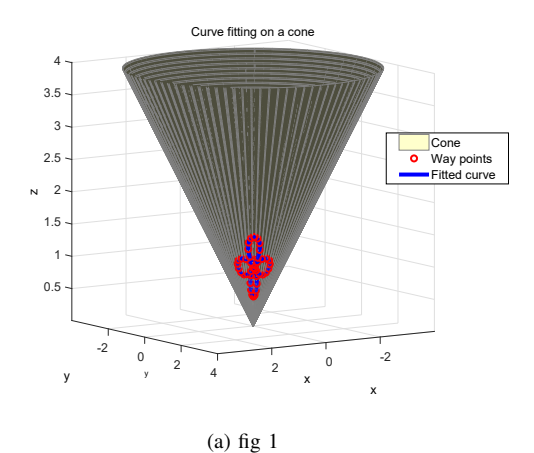
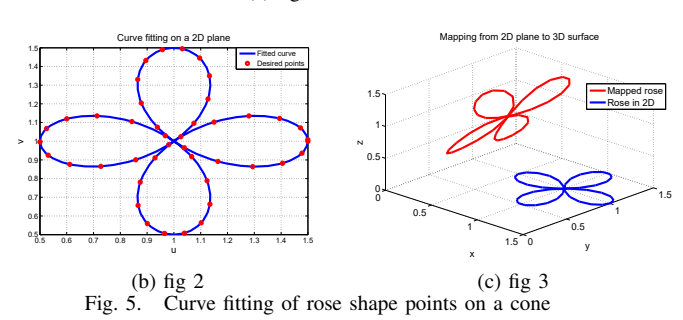


Fig. 4. Pattern placement of a square spiral on a cone with boundary and visiting points condition





Error value $E_c\approx 10^{-7}$ rad, $E_i\approx 10^{-6}$ cm, as (22) is an isometric and conformal parametrization. The condition error is $E_{cd}\approx 10^{-3}$ cm.

IV. CURVE FITTING ON A MANIFOLD

In this section, we no longer deal with an original pattern in 2D. However, we are dealing directly with some points on the manifold [17], and the task is to find a curve or pattern which pass through the points. Let S be a two dimensional manifold in \mathbb{R}^3 , with implicit Cartesian coordinates function f(x, y, z) = 0. This surface can be parametrized $S:(u,v)\in\mathbb{R}^2\to\mathbb{R}^3$. As there is a mapping between the surface and the (u, v) plane, the curve fitting problem can be investigated in \mathbb{R}^2 . For a set of points on the plane $P = \{p_i, i = 1, ..., n\} \in (u, v), \text{ there is } q_i = S(p_i), \text{ where } i \in \{p_i, i = 1, ..., n\} \in \{p_i, i = 1, ..., n\}$ q_i are 3D points on the manifold. A curve fitting algorithm should find a curve on manifold to pass through q_i . If the points q_i are given directly, we need to first compute the corresponding point p_i in (u, v) [18]. After generating p_i , the curve fitting problem is simplified to 2D, and a curve $r_{cp} = [u(\theta), v(\theta)]$ can be approximated. As the manifold is known, $r_s(u, v) = [x(u, v), y(u, v), z(u, v)]$ can be obtained. In Fig. 5 a, one can see red points on the cone as q_i . In b, red dots are p_i which are corresponding planar points of q_i . A cubic spline interpolation with end condition is applied to obtain curve fitting on 2D (in blue). After the planar curve fitting, the curve is mapped into the cone by $r_s(u, v)$. Both shapes can be seen in part (c).

V. EXPERIMENTAL VALIDATION

We conducted a series of experiments mapping constrained patterns onto a 3D surface to verify our approach. We used a



Fig. 6. Lulzbot Taz 5 3D printer



(a) fig 1 (b) fig 2 Fig. 7. Printing different constrained patterns on the sphere

Lulzbot Taz 5 3D printer (Fig. 6), which was mounted with a 0.5mm nozzle, to create a 3D surface as well as deposit polymer materials in the desired pattern. The surface was a hemisphere developed in Creo Parametric, with a radius of 1.5 inches (38.1 mm), printed using clear ABS plastic. The center of the sphere was known with respect to 3D printer's coordinate system.

We mapped a planar rose and spiral pattern onto the sphere. Equation (17) is used for stereographic mapping, and K was optimized to make the pattern to pass over desired points. For the spiral pattern, the desired points are

$$\begin{bmatrix} 2.7 \\ -11.2 \\ 36.3 \end{bmatrix} \begin{bmatrix} 9.24 \\ -0.45 \\ 37 \end{bmatrix} \begin{bmatrix} -0.44 \\ 7 \\ 37.5 \end{bmatrix} \begin{bmatrix} 0 \\ 0 \\ 38.1 \end{bmatrix}.$$

For the rose, the way points are

$$\begin{bmatrix} 1.78 \\ -20.33 \\ 31.18 \end{bmatrix} \begin{bmatrix} 18.71 \\ 5.87 \\ 32.67 \end{bmatrix} \begin{bmatrix} -4.61 \\ 19.46 \\ 32.4 \end{bmatrix} \begin{bmatrix} -24.66 \\ 1.82 \\ 28.99 \end{bmatrix}.$$

After the 3D patterns were generated, we sampled 130 evenly spaced points on each pattern. These points were used to generate g-code, which specifies locations for the nozzle, along with specified extrusion and feed rates. Fig.7 shows the rose and spiral pattern on the sphere after printing.

Red squares represents desired points to be passed. It can be observed that 3D patterns were successfully mapped onto the sphere with minimal distortion. In addition, patterns passed over the desired way points.

Note that the 3D printer maintains a constant orientation of the nozzle downward, and the nozzle is notably wider than the extrusion orifice. Therefore, while the portions of the patterns near the side of the sphere were printed correctly, they smeared in some points due to the contact by the wide nozzle. This problem hinders us from conducting experiments on the side of the sphere or on surfaces with more curvature. This indicates that it is necessary to keep the nozzle normal to the surface, which is an avenue of our research using articulated robot arms [19].

VI. CONCLUSIONS AND FUTURE WORK

This paper investigated mapping a desired 2D pattern onto a 3D curved surface with minimum distortion. Additional goals were considered, such as ensuring the pattern passes through specific way points on the surface and remains bounded in a specific region. To address this problem, an optimization-based planar transformation along with surface parametrization are employed. Simulations and experiments were presented for different patterns mapped to different surfaces, which showed the performance of our approach.

This work fits into our larger goal of printing arbitrary patterns onto arbitrary curved surfaces. There are several avenues of concurrent and future work. The methods presented here will be extended to general smooth surfaces. We are working on 3D vision methods to fit a surface to a given object to plan trajectories. We are also developing motion planning and control of deposition nozzles mounted on a robot end effector to keep it normal with the surface, as well as our past work on adaptive control to regulate the flow/deposition rate to regulate line width and prevent drips.

REFERENCES

- E. Galceran and M. Carreras, "A survey on coverage path planning for robotics," *Robotics and Autonomous Systems*, vol. 61, no. 12, pp. 1258–1276, 2013.
- [2] E. Horvátha, C. Pozna, and R.-E. Precup, "Robot coverage path planning based on iterative structured orientation," *Acta Polytechnica Hungarica*, vol. 15, no. 2, 2018.
- [3] C. Di Franco and G. C. Buttazzo, "Energy-aware coverage path planning of uavs.," in *IEEE International Conference on Autonomous Robot Systems and Competitions*, pp. 111–117, 2015.
- [4] T. Oksanen and A. Visala, "Coverage path planning algorithms for agricultural field machines," *Journal of Field Robotics*, vol. 26, no. 8, pp. 651–668, 2009.
- [5] F. Yasutomi, M. Yamada, and K. Tsukamoto, "Cleaning robot control," in *IEEE International Conference on Robotics and Automation*, pp. 1839–1841, 1988.
- [6] M. Bosse, N. Nourani-Vatani, and J. Roberts, "Coverage algorithms for an under-actuated car-like vehicle in an uncertain environment," in *IEEE International Conference on Robotics and Automation*, pp. 698– 703, 2007.
- [7] Z. L. Cao, Y. Huang, and E. L. Hall, "Region filling operations with random obstacle avoidance for mobile robots," *Journal of Robotic Systems*, vol. 5, no. 2, pp. 87–102, 1988.
- [8] P. N. Atkar, A. Greenfield, D. C. Conner, H. Choset, and A. A. Rizzi, "Uniform coverage of automotive surface patches," *The International Journal of Robotics Research*, vol. 24, no. 11, pp. 883–898, 2005.

- [9] P. Hertling, L. Hog, R. Larsen, J. W. Perram, and H. G. Petersen, "Task curve planning for painting robots. i. process modeling and calibration," *IEEE Transactions on Robotics and Automation*, vol. 12, pp. 324–330, April 1996.
- [10] B. H. Jafari, N. Lee, B. Antohe, and N. Gans, "Parameter estimation and line width control of robot guided inkjet deposition," in *American Control Conference*, pp. 918–924, June 2018.
- [11] H. Biermann, I. Martin, F. Bernardini, and D. Zorin, "Cut-and-paste editing of multiresolution surfaces," in ACM Transactions on Graphics, vol. 21, pp. 312–321, 2002.
- [12] V. Kraevoy and A. Sheffer, "Template-based mesh completion.," in Symposium on Geometry Processing, vol. 385, pp. 13–22, 2005.
- [13] Y. Lin, C. Ni, N. Lei, X. D. Gu, and J. Gao, "Robot coverage path planning for general surfaces using quadratic differentials," in *IEEE International Conference on Robotics and Automation*, pp. 5005–5011, May 2017.
- [14] M. P. Do Carmo, Differential Geometry of Curves and Surfaces: Revised and Updated Second Edition. Courier Dover Publications, 2016
- [15] M. S. Floater and K. Hormann, "Surface parameterization: a tutorial and survey," in *Advances in multiresolution for geometric modelling*, pp. 157–186, Springer, 2005.
- [16] H. Choset, "Coverage of known spaces: The boustrophedon cellular decomposition," *Autonomous Robots*, vol. 9, no. 3, pp. 247–253, 2000.
- [17] S. Flöry and M. Hofer, "Constrained curve fitting on manifolds," Computer-Aided Design, vol. 40, no. 1, pp. 25–34, 2008.
- [18] S.-M. Hu and J. Wallner, "A second order algorithm for orthogonal projection onto curves and surfaces," *Computer Aided Geometric Design*, vol. 22, no. 3, pp. 251–260, 2005.
- [19] B. H. Jafari, L. Namhyung, R. Thompson, J. Schellhorn, B. Antohe, and N. Gans, "A robot system for automated wound filling with jetted materials," in 2018 IEEE/RSJ International Conference on Intelligent Robots and Systems (IROS), pp. 1789–1794, Oct 2018.